J|A|C|S ARTICLES

Published on Web 08/28/2009

Spectroscopic Identification of the Resonance-Stabilized *cis*- and *trans*-1-Vinylpropargyl Radicals

Neil J. Reilly, Masakazu Nakajima, Tyler P. Troy, Nahid Chalyavi, Kieran A. Duncan, Klaas Nauta, Scott H. Kable, and Timothy W. Schmidt*

School of Chemistry, The University of Sydney, NSW 2006, Australia

Received June 4, 2009; E-mail: t.schmidt@chem.usyd.edu.au

Abstract: The *cis*-1-vinylpropargyl (*cis*-1VPR, *cis*-pent-4-en-1-yn-3-yl) and *trans*-1-vinylpropargyl (*trans*-1VPR, *trans*-pent-4-en-1-yn-3-yl) radicals, produced in a supersonically cooled hydrocarbon discharge, have been identified by a synergy of 2-dimensional fluorescence and ionization spectroscopies, revealing their electronic origin transitions at 21 232 and 21 645 cm^{-1} respectively. These assignments are supported by an excellent agreement between calculated ground state frequencies of *cis*-1VPR and *trans*-1VPR with those obtained by dispersed fluorescence spectroscopy. In addition, high-resolution rotational contours of the two bands are well simulated using calculated $\tilde{X}$- and $\tilde{A}$-state *trans*-1VPR and *cis*-1VPR rotational constants. Finally, computed origin transition energies of these two isomers are within several hundred wavenumbers of the observed band positions. With the 1-phenylpropargyl radical, the 1VPR isomers are the second 1-substituted propargyl species to have been observed abundantly from a hydrocarbon discharge, while no 3-substituted analogue has been positively identified. This is likely due to the greater resonance stabilization energy of the 1-substituted species, arising from concerted delocalization of the unpaired electron over the vinyl and propargyl moieties.

Introduction

Resonance-stabilized radicals (RSRs) are known to persist as reaction intermediates in the chemistries of combustion,[1,2] planetary atmospheres,[3−6] and circumstellar shells.[7] RSRs possess an unpaired electron that is delocalized over several sites. Consequently, they are stabilized with respect to their reaction products with stable molecules and are formed preferentially from the decomposition of stable hydrocarbons, causing them to reach high concentrations in flames.[8−10] Indeed, the propargyl radical is widely believed to build up to concentrations so high that its self-reaction becomes significant and leads to the formation of benzene and subsequently higher aromatics.[1,2] Propargyl radical thus stands accused of contributing to the pollution caused by combustion of hydrocarbons and is also implicated in the formation of benzene and subsequently tholins in the atmosphere of Titan,[3−6] the largest moon of Saturn.

Benzene formation appears to be the rate-determining step in the formation of polycyclic aromatic hydrocarbons (PAHs), which in terrestrial combustion pose significant environmental and health concerns.[11−13] In circumstellar envelopes they are thought to be sites of nucleation for dust grains,[14] and in Titan's atmosphere have been shown theoretically to provide a major pathway for aerosol production.[5] Interest in the latter has been piqued by the recent detection of PAHs with the Cassini Plasma Spectrometer.[3,4]

All of the major benzene formation routes from smaller species involve RSRs; the dominant pathway, involving the recombination of two propargyl radicals, is well-known,[1,2,15−18] whereas lesser but still important channels involving addition of acetylene to C_4H_3/C_4H_5[9,19−21] and addition of methyl radical to C_5H_5[22−25] have been less thoroughly characterized, in part because of the wider variety of isomers possible.

(1) McEnally, C. S.; Pfefferle, L. D.; Atakan, B.; Kohse-Hinghaus, K. *Prog. Energy Combust. Sci.* **2006**, *32*, 247.
(2) Richter, H.; Howard, J. B. *Prog. Energy Combust. Sci.* **2000**, *26*, 565.
(3) Waite jr, J. H.; Young, D. T.; Cravens, T. E.; Coates, A. J.; Crary, F. J.; Magee, B.; Westlake, J. *Science* **2007**, *316*, 870.
(4) Atreya, S. *Science* **2007**, *316*, 843.
(5) Lebonnois, S. *Planet. Space Sci.* **2005**, *53*, 486.
(6) Wilson, E. H.; Atreya, S. K.; Coustenis, A. *J. Geophys. Res.-Planets* **2003**, *108* (E2), 5014.
(7) Cherchneff, I.; Barker, J. R.; Tielens, A. G. G. M. *Astrophys. J.* **1992**, *401*, 269.
(8) Miller, J. A. *Proc. Combust. Inst.* **1996**, *20*, 461.
(9) Miller, J. A.; Melius, C. F. *Combust. Flame* **1992**, *91*, 21.
(10) Melius, C. F. *Proc. Combust. Inst.* **1992**, *24*, 621.
(11) Hansen, J.; Sato, M.; Ruedy, R.; Lacis, A.; Oinas, V. *Proc. Natl. Acad. Sci. U.S.A.* **2000**, *97*, 9875.
(12) Denissenko, M. F.; Pao, A.; Tang, M. S.; Pfeifer, G. P. *Science* **1996**, *274*, 430.
(13) Durant, J. L.; Busby, W. F.; Lafleur, A. L.; Penman, B. W.; Crespi, C. L. *Mutat. Res.* **1996**, *371*, 123.
(14) Keller, R.; Sedlmayr, E. *Mitt. Astron. Ges.* **1983**, *60*, 312.
(15) Kern, R. D.; Singh, H. J.; Wu, C. H. *Int. J. Chem. Kinet.* **1988**, *20*, 731.
(16) Miller, J. A.; Klippenstein, S. J. *J. Chem. Phys. A* **2001**, *105*, 7254.
(17) Atakan, B.; Hartlieb, A. T.; Brand, J.; Kohse-Hinghaus, K. *Proc. Combust. Inst.* **1998**, *27*, 435.
(18) Hoyermann, K.; Mauβ, F.; Zeuch, T. *Phys. Chem. Chem. Phys.* **2004**, *6*, 3824.
(19) Atakan, B.; Lamprecht, A.; Kohse-Hinghaus, K. *Combust. Flame* **2003**, *133*, 431.
(20) Hansen, N.; Klippenstein, S. J.; Miller, J. A.; Wang, J.; Cool, T. A.; Yang, B.; Yang, R.; Wei, L.; Huang, C.; Wang, J.; Qi, F.; Law, M. E.; Westmoreland, P. R. *J. Phys. Chem A* **2006**, *110*, 3670.
(21) Walch, S. P. *J. Chem. Phys.* **1995**, *103*, 8544.
(22) Ikeda, E.; Tranter, R. S.; Kiefer, J. H.; Kern, R. D. *Proc. Combust. Inst.* **2000**, *28*, 1725.

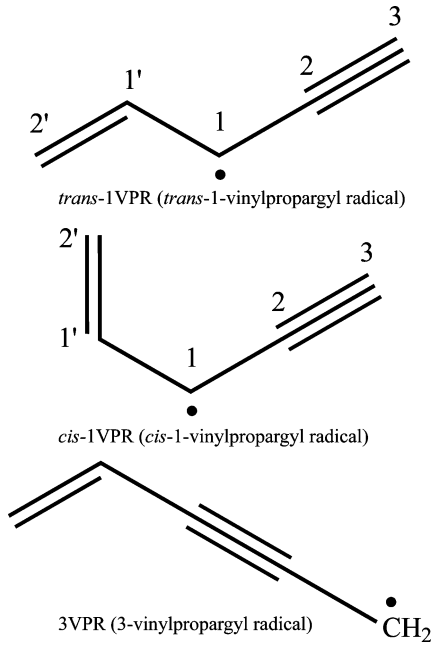

Figure 1. Lewis structures of vinylpropargyl radicals relevant to this work.

In addition to its postulated importance to benzene formation, the cyclopentadienyl radical, *c*-C_5H_5, is considered to be the key intermediate in naphthalene formation by radical recombination.[22−24,26,27] However, while *c*-C_5H_5 represents the global minimum on the C_5H_5 potential energy surface,[28] a linear isomer has been observed in photoionization efficiency (PIE) spectra of flames of several precursors including benzene and has been assigned by Franck−Condon simulations as the 1-vinylpropargyl radical (1VPR).[29−32] Furthermore, C_5H_5 species attributed to 1VPR and 3-vinylpropargyl (3VPR) radicals have been observed from the reaction of ground state (^3P) carbon atoms with 1,3-butadiene in a crossed molecular beam experiment, with 1VPR favored by a factor of 8.[33] However, despite these reports, neither 1VPR nor 3VPR has been identified spectroscopically. These two radicals, shown in Figure 1, are the next most stable C_5H_5 isomers,[28,33] with calculated energies some 122 (1VPR) and 136 kJ/mol (3VPR) above *c*-C_5H_5.

Decomposition of *c*-C_5H_5 via 1VPR has been shown to contribute nearly half of all propargyl radicals in cyclopentene combustion.[25] Thus, 1VPR is a substituted propargyl radical that is a potentially important source and sink of propargyl radicals in combustion; and further, in the atmosphere of Titan, where, intriguingly, unidentified species have been detected by the *Cassini* INMS at $m/z = 65$.[3,34]

It is in this broad context that we have recently been studying radicals formed in supersonically cooled discharges of hydrocarbon precursors by a synergy of spectroscopic techniques, facilitated greatly by two-dimensional fluorescence (2DF) excitation/emission spectroscopy.[35] Recently we reported the detection by 2DF of the resonance-stabilized 1-phenylpropargyl radical, which proved to be the most conspicuous species in the fluorescence spectroscopy of the benzene discharge after the ubiquitous C_2, C_3 and CH radicals.[36]

In this work, we present a 2DF spectrum in the excitation wavelength range 448−474 nm of the products of an electrical discharge containing 1-hexyne (which itself contains the propargyl moiety), which exhibits spectral signatures of two unidentified species. High-resolution laser-induced fluorescence (LIF) rotational profiles and dispersed fluorescence (DF) spectra of the apparent origin transitions of these band systems, at 462 and 471 nm, are presented. Resonant 2-color 2-photon ionization spectroscopy confirms the carriers as having the molecular formula C_5H_5. We perform electronic structure calculations on the 1- and 3-vinylpropargyl radicals, for simulation of the observed rotational profiles and comparison of the calculated vibrational frequencies with those obtained from DF spectra. This has allowed the definite assignment of the 462 and 471 nm bands to the *trans*-1VPR and *cis*-1VPR radicals respectively, providing valuable probe wavelengths for these important reactive intermediates. A discussion of the large resonance stabilization energies of these radicals, based on changes in bond lengths and vibrational frequencies between each radical and its molecular parent, is presented.

Experimental Section

The apparatus used in this experiment have been described elsewhere.[36,37] Briefly, a pulsed discharge nozzle (PDN) was used to produce the radicals of interest from 1-hexyne (Fluka, ≥ 99%) at room temperature vapor pressure seeded in argon. A 1.8 kV voltage pulse of of 35 μs duration was applied to the outer electrode of the PDN through a 15 kΩ ballast resistor, timed to strike during the gas pulse. Typical operating pressure throughout the experiment was 2×10^{-4} Torr with a stagnation pressure of 7 bar. In fluorescence experiments, the molecular beam was interrogated approximately 2 cm downstream of the nozzle orifice with the output of an XeCl Excimer or Nd:YAG pumped dye laser containing Coumarin 460 dye.

A two-dimensional fluorescence (2DF) spectrum was recorded by the method outlined previously.[35] An intensified charge-couple device array (iCCD) was mounted to the exit aperture of an optical spectrograph and exposed for 50 shots per laser wavelength step. A background image, also exposed for 50 shots with the discharge on but the laser absent, was subtracted from each signal image to minimize the intrusion of non-laser-dependent emission from electronically excited discharge products such as C_2 and C_3. For high-resolution measurements of rotational contours of subsequently observed bands, the dye laser was used with an intracavity etalon, giving a minimum spectral line width of 0.04 cm^{-1}. Absolute frequency calibration of the laser was obtained using a wavemeter.

(23) Moskaleva, L. V.; Mebel, A. M.; Lin, M. C. *Proc. Combust. Inst.* **1996**, *26*, 521.
(24) Melius, C. F.; Colvin, M. E.; Marinov, N. M.; Pitz, W. J.; Senkan, S. M. *Proc. Combust. Inst.* **1996**, *26*, 685.
(25) Lindstedt, R. P.; Rizos, K.-A. *Proc. Combust. Inst.* **2002**, *29*, 2291.
(26) Marinov, N. M.; Pitz, W. J.; Westbrook, C. K.; Vincetore, A. M.; Castaldi, M. J.; Senkan, S. M.; Melius, C. F. *Combust. Flame* **1998**, *114*, 192.
(27) Dean, A. M. *J. Phys. Chem.* **1990**, *94*, 1432.
(28) Moskaleva, L. V.; Lin, M. C. *J. Comput. Chem.* **1999**, *21*, 415.
(29) Yang, B.; Huang, C.; Wei, L.; Wang, J.; Sheng, L.; Zhang, Y.; Qi, F.; Zheng, W.; Li, W.-K. *Chem. Phys. Lett.* **2006**, *423*, 321.
(30) Huang, C.; Wei, L.; Yang, B.; Wang, J.; Li, Y.; Sheng, L.; Zhang, Y.; Qi, F. *Energy Fuels* **2006**, *20*, 1505.
(31) Hansen, N.; Klippenstein, S. J.; Miller, J. A.; Wang, J.; Cool, T. A.; Law, M. E.; Westmoreland, P. R.; Kasper, T.; Kohse-Hinghaus, K. *J. Phys. Chem A* **2006**, *110*, 4376.
(32) Hansen, N.; Kasper, T.; Klippenstein, S. J.; Westmoreland, P. R.; Law, M. E.; Taatjes, C. A.; Kohse-Hinghaus, K.; Wang, J.; Cool, T. A. *J. Phys. Chem A* **2007**, *111*, 4081.
(33) Hahndorf, I.; Lee, H. Y.; Mebel, A. M.; Lin, S. H.; Lee, Y. T.; Kaiser, R. I. *J. Chem. Phys.* **2000**, *113*, 9622.
(34) Cravens, T. E.; et al. *Geophys. Res. Lett.* **2006**, *33*, L07105.
(35) Reilly, N. J.; Schmidt, T. W.; Kable, S. H. *J. Phys. Chem.* **2006**, *23*, 85.
(36) Reilly, N. J.; Kokkin, D. L.; Nakajima, M.; Nauta, K.; Kable, S. H.; Schmidt, T. W. *J. Am. Chem. Soc.* **2008**, *130*, 3137.
(37) Terentis, A. C.; Stone, M.; Kable, S. H. *J. Phys. Chem.* **1994**, *98*, 10802.

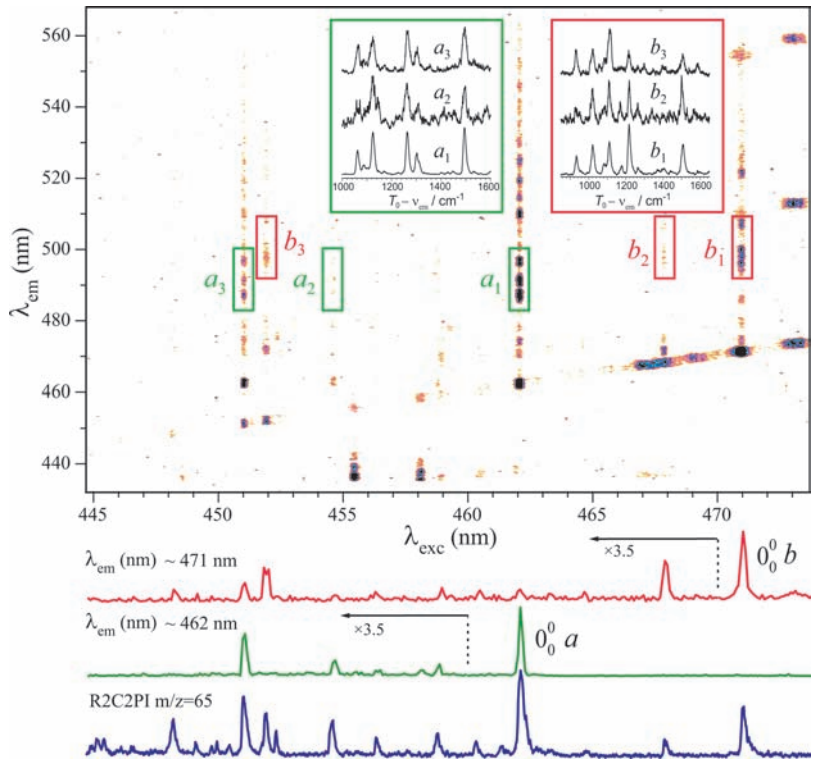

Figure 2. 2DF spectrum of a 1-hexyne discharge in the region $445 \leq \lambda_{exc} \leq 474$ nm and $432 \leq \lambda_{em} \leq 568$ nm. Most of the strong features along the resonance fluorescence line $\lambda_{exc} = \lambda_{em}$ in the region $\lambda_{exc} = 467-474$ nm are due to C_2 Swan bands. Features due to hot bands of the "comet" band system of C_3 can be seen, for example, near (455, 437) and (458, 437). The boxes a_1-a_3 and b_1-b_3 highlight the emission spectral "fingerprints" of the strongest unidentified features, which as shown in higher resolution in the insets can be ascribed to two distinct species. Coarse LIF spectra of these two species, obtained from the emission wavelengths 462 nm (a) and 471 nm (b) (the apparent origin transitions), are displayed beneath. A R2C2PI spectrum at $m/z = 65$ is shown beneath the LIF spectra.

For detailed fluorescence experiments, the emission was imaged onto the entrance slit of a 0.75 m Spex monochromator. To minimize intrusion of scattered laser light and fluorescence from C_2 and C_3 during high-resolution LIF scans, the monochromator was fixed at approximately 2030 cm^{-1} to the red of the laser, with 3 mm slits corresponding to a 60 cm^{-1} fwhm bandpass. This permitted detection of emission to the acetylenic stretching mode of 1VPR, which is strongly active upon electronic excitation, while easily avoiding C_2 and C_3 emission features. For dispersed fluorescence, the laser was fixed to the maxima of the rotational profiles and the monochromator was scanned with 0.1−0.5 mm slits, corresponding to a spectral resolution of 2−10 cm^{-1}. Fluorescence was detected by a photomultiplier tube mounted at the monochromator exit. The fluorescence decay profile was viewed on an oscilloscope and integrated with a gated boxcar averager. The digitized output was recorded on a personal computer.

Resonant 2-color 2-photon ionization (R2C2PI) spectroscopy was performed to confirm the masses of the carriers of the observed bands. The apparatus, a two-stage differentially pumped vacuum chamber, was identical to that used previously to identify the 1-phenylpropargyl radical.[36] Briefly, a skimmed molecular beam containing products of a discharge of hexyne in argon, as above, was probed between the extraction grids of a time-of-flight (TOF) tube by the coincident pulses of a scanned OPO laser and a frequency quadrupled Nd:YAG laser (266 nm). The positive ions were extracted vertically and perpendicularly to the laser and molecular beam into the TOF tube. Ion signal at $m/z = 65$ was viewed on a digital oscilloscope and integrated as a function of laser wavelength.

Results

Figure 2 shows a 2DF spectrum of a discharge containing 1-hexyne in the region $445 \leq \lambda_{exc} \leq 474$ nm and $432 \leq \lambda_{em} \leq 568$ nm. The notation (λ_{exc}, λ_{em}) is used to locate particular features according to their excitation and emission wavelengths.[35] The short emission spectra originating at (455, 437) and (458, 437) are due to hot bands of the "comet" band system of C_3. There are several strong features along the $\lambda_{exc} = \lambda_{em}$ resonance fluorescence line between $\lambda_{exc} = 468$ and 474 nm. Most of these are $\Delta v = +1$ Swan transitions of C_2.

The great advantage of 2DF is that it provides an overview that allows one to immediately see new species that in excitation or emission alone are either not obvious or are obscured by comet and Swan bands. Many other spectral features are clearly not due to C_2 or C_3, with the strongest of these at (462, 462) and (471, 471). As is highlighted in the boxes a_1 and b_1, these bands clearly have different emission "fingerprints" and therefore do not have a common carrier. Even at the low resolution of the 2DF spectrum, the a_1 fingerprint is evident in the emission spectra from 454.6 nm (a_2) and 450.8 nm (a_3), and similarly, the boxes b_2 and b_3 exhibit the b_1 fingerprint. All of the unassigned spectral features can thus be ascribed to two species. This is made abundantly clear in the insets, which contain higher resolution dispersed fluorescence spectra of the boxed fingerprint regions, measured with a conventional scanning monochromator and photomultiplier. In the *a*-inset, the abscissa indicates wavenumber relative to the energy of the apparent origin transition (at 462 nm), and in the *b*-inset it is measured relative to the 471 nm feature; in the spectra a_1 and b_1, the abscissa therefore indicates the ground state vibrational frequency, showing that each carrier contains several active vibrational modes around 900−1300 cm^{-1}, which are important to their later identification. In each band system, the strongest emission

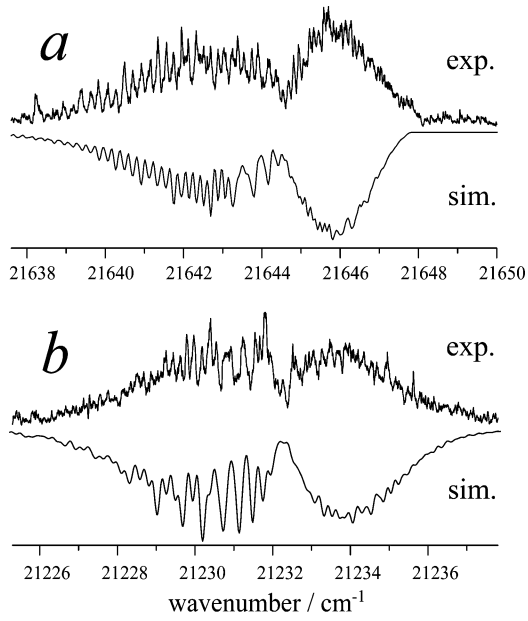

Figure 3. High-resolution LIF rotational profiles of two species formed in a 1-hexyne discharge, absorbing at 462 and 471 nm, respectively, each with a simulated contour reflected beneath. The simulations are not fit but rather are based on calculations. They are discussed in the text (parameters in Table 2).

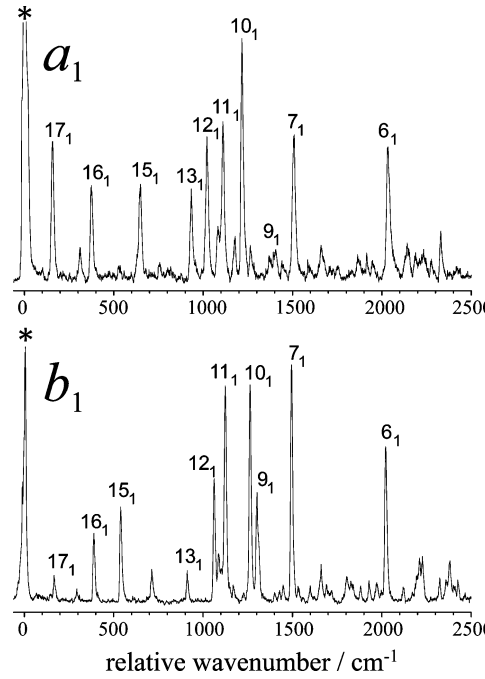

Figure 4. High-resolution dispersed fluorescence (DF) spectra of two species formed in a 1-hexyne discharge, absorbing at 462 nm (a_1) and 471 nm (b_1). The assignments are discussed in the text.

occurs at the wavelength of the origin transition. Coarse resolution LIF spectra of each species, which with a monochromator and photomultiplier would be exceedingly difficult to obtain without prior knowledge of an appropriate fluorescence detection wavelength, can be extricated from the 2DF spectrum by plotting the fluorescence intensity at the origin wavelengths as a function of λ_{exc}. Shown beneath the 2D spectrum, these spectra exhibit minimal intrusion by each other and from C_2 and C_3, and are dominated by the origin transitions by a factor of at least three, indicating the "vertical" nature of the electronic transition.

The R2C2PI spectrum of the products of a discharge identical to that performed in the fluorescence experiments is displayed at the bottom of Figure 2. All of the major features of spectrum *a* and spectrum *b* are reproduced by the signal monitored at $m/z = 65$, indicating both spectra to be due to species of molecular formula C_5H_5.

To properly identify the carriers of the unassigned features in the 2DF spectrum, the 462 and 471 nm bands were studied in more detail using conventional fluorescence spectroscopy. High resolution LIF rotational profiles of each band are shown in Figure 3, plotted against excitation wavenumber, with the labels *a* and *b* retained from the coarse resolution LIF spectra in Figure 2. Reflected beneath each contour are simulated profiles obtained using calculated molecular constants of candidate carriers (vide infra). Dispersed fluorescence (DF) spectra of each band, portions of which appear in the insets in Figure 2 as a_1 and b_1 and which retain those labels, are shown in full in Figure 4, plotted against displacement from the pump laser frequency. The DF spectra are quite similar: each has a low frequency band around 130−170 cm^{-1}, five strong bands around 900−1300 cm^{-1}, and strong bands at 1500 and 2030 cm^{-1}. The simulations of the rotational profiles and, more importantly, the assignments of the DF spectra form much of the basis of of the identification of each of these C_5H_5 species, detailed in the next section.

Theoretical Methods

Density functional theory (DFT) was employed to calculate ground state frequencies and geometries of candidate band carriers using the B3LYP functional and the 6-311+G(d,p) basis within the Gaussian 03 suite of electronic structure programs.[38] This level of theory, with frequencies scaled by 0.97, was found previously to reproduce experimental ground state frequencies exceptionally well for this class of molecule.[36] To investigate the electronic transitions of candidates, calculations were performed with the Molpro package.[39] Ground and excited state geometries of 1VPR and 3VPR were calculated by CASSCF/6-31G(d) with an active space of seven electrons in seven π orbitals. Multireference configuration interaction (MRCI) calculations were performed using the CASSCF wave functions as a reference to estimate the energies of electronic transitions.

Discussion

Identification of the Spectral Carriers. *trans*-1-Vinylpropargyl Radical. We concentrated initially on determining the carrier of the 462 nm band (a_1), which was also detected by Ding et al.,[40] in a R2C2PI spectrum of a jet-cooled benzene discharge, in the $m/z = 65$ channel. They used DFT to investigate the energies, ground state rotational constants, and vertical transition energies T_e of six candidates, 1VPR and 3VPR among them, to reconcile with experiment. The 462 nm band was assigned to 3VPR on the basis of a combination of its superior *a*-type rotational profile simulation using their calculated rotational constants, closeness of the computed T_e to experiment, and low relative energy. Another band observed, near 450.8 nm, was ascribed to pentamethylidene, a planar "w"-

(38) Frisch, M. J.; et al. *Gaussian 03, Revision C.02*; Gaussian, Inc.: Wallingford, CT, 2004.
(39) Werner, H.-J.; et al. MOLPRO, version 2000.1, a package of ab initio programs, 2000; see http://www.molpro.net.
(40) Ding, H.; Boguslavskiy, A. E.; Maier, J. P. *Phys. Chem. Chem. Phys.* **2005**, *7*, 888.

Table 1. Comparison of Experimental (from DF Spectra a_1 and b_1) and Calculated (B3LYP/6-311+G(d,p)) Frequencies of Relevant a' Modes of *trans*-1VPR, *cis*-1VPR, and 3VPR[a]

mode	description	*trans*-1VPR, DF a_1	*trans*-1VPR, theory × 0.97	*cis*-1VPR, DF b_1	*cis*-1VPR, calcd × 0.97	3VPR, calcd × 0.97
ν_{17}	propargyl/vinyl wag	169	169	155	153	138
ν_{16}	C(2′)C(1′)C(1) + C(1)C(2)C(3) bend	390	387	373	372	322
ν_{15}	C(1′)C(1)C(2) + C(1)C(2)C(3) bend	540	540	642	632	523
ν_{14}	acetylenic H bend		654		653	746
ν_{13}	C(1′)C(1)C(2) bend/symmetric stretch	910	898	932	914	1010
ν_{12}	C(1′)C(1) + C(1)C(2) antisymmetric stretch	1064	1064	1019	1006	1041
ν_{11}	C(1′)C(2′) + C(1′)C(1) antisymmetric stretch	1127	1165	1111	1124	1247
ν_{10}	C(2′)C(1′)C(1) bend/symmetric stretch	1265	1249	1217	1221	1278
ν_9	C(2′)C(1′)C(1) + C(1′)C(1)C(2) bend/stretch	1304	1292	1396	1372	1400
ν_8	in-plane H bend		1423		1390	1454
ν_7	C(1′)C(2′) stretch	1496	1494	1503	1495	1526
ν_6	C(2)C(3) stretch	2024	2021	2032	2037	1985

[a] All theoretical frequencies presented have been scaled by 0.97. Labeling of atoms follows Figure 1. Mode descriptions are based on *trans*-1VPR; *cis*-1VPR modes are almost completely analogous. The frequencies of these modes are compared with those of their nearest a' 3VPR analogues. Modes 1−5 (not shown) are the C−H stretches.

shaped C_5H_5 isomer. However, it is clear from the 2DF spectrum (Figure 2) that this band (a_3) has the same carrier as the 462 nm band (a_1). As such, we put the previous assignment aside in deference to the data reported here, which as will be shown, definitively argues for a reassignment of these bands.

The ground state vibrational frequencies of a benzene discharge product absorbing at 476 nm, with molecular mass 115, were crucial to its identification in our laboratory as the 1-phenylpropargyl radical, ahead of several other isomers, including the 3-phenylpropargyl radical.[36] As such, we have reason to suspect that 1VPR may be formed in preference to the 3VPR isomer, and thus it is appropriate to review the assignment of the 462 nm band to 3VPR. We use the dispersed fluorescence spectrum a_1, from the 462 nm band, to guide our selection of candidate C_5H_5 isomers for further consideration. A vital clue that allows the elimination of many isomers is the presence of the strong band at ∼2030 cm^{-1}, characteristic of an acetylenic stretching mode. Sensible candidates should therefore include those isomers that contain a C≡C bond. It is further proposed that, of the isomers satisfying this criterion, only those that are also resonance-stabilized should be considered. Several recent experimental results show that this is a sensible proposition. First, as was mentioned in the introduction, PIE spectra at $m/z = 65$ of flames of several precursors, including benzene (from which the 462 nm carrier was first observed in a discharge)[40] have been attributed to perhaps as few as two isomers, *c*-C_5H_5 and 1VPR, both of which are resonance-stabilized. Further, in the reaction of carbon atoms with butadiene in a crossed-beam experiment, 1VPR and 3VPR were the only products observed, with the former favored by a factor of 8.[33] Thus, RSRs can prevail in the low temperatures of a molecular beam as well as in the high temperatures of combustion, both of which are effected in the jet-cooled discharge source. Additionally, it should be borne in mind that the carrier here has been formed from a low-current discharge of 1-hexyne and thus likely contains an unbranched backbone.

With this in mind and with respect to the prevailing assignment of the 462 nm feature to 3VPR by Ding et al.,[40] calculations were performed on the remaining candidates, 1VPR and 3VPR (Figure 1), to aid interpretation of the DF spectra and simulation of the rotational profiles. It should be pointed out that 1VPR exists in the *cis* and *trans* conformations, related by a 180° rotation of the vinyl moiety about the C(1)−C(1′) bond (see Figure 1). The two isomers were first identified by electron spin resonance (ESR) following hydrogen abstraction of pent-4-en-1-yne by *tert*-butoxy.[41] The energy difference between them was measured to be 1.2 kJ/mol, with the barrier height to rotation about the C(1)−C(1′) bond some 54 kJ/mol.[42] We calculated ground state geometries and frequencies for *trans*-1VPR, *cis*-1VPR, and 3VPR. All harmonic frequencies calculated at the optimized geometries were found to be real. Table 1 lists the frequencies of the strongest observed bands from DF spectra a_1 and b_1 with the DFT frequencies of the relevant a' modes of *trans*-1VPR, *cis*-1VPR, and 3VPR, scaled by 0.97.

The lowest frequency modes, being the most readily assigned, provide the surest identification of the spectral carrier. Ground and excited state geometries of 1VPR and 3VPR calculated by CASSCF indicate that the greatest geometry change following electronic excitation involves C−C bond lengths. Specifically, in all three radicals, three C−C bonds lengthen, particularly the vinyl double bond and propargyl triple bonds, and one shortens (C(1)−C(2) in 1VPR). In addition, there are some small changes to some of the CCC bond angles. Consequently, of the a' modes, the acetylenic and vinylic stretching modes (ν_6 and ν_7 respectively), and the carbon backbone bend−stretch modes ν_{9-13} should dominate the spectra, while some weak activity in the a' bending modes ν_{15-17} might be expected, an analysis that is largely borne out in Figure 4. In DF spectrum a_1, there are bands at 169, 390, and 540 cm^{-1} relative to the laser frequency. These are in excellent agreement with the calculated a' frequencies $\nu_{17} = 169$ cm^{-1}, $\nu_{16} = 387$ cm^{-1}, and $\nu_{15} = 540$ cm^{-1} of *trans*-1VPR. In addition, the remainder of the strong bands in spectrum a_1 are generally within much less than 2% of the calculated frequencies of the expected Franck−Condon active a' modes of *trans*-1VPR. Most of the weaker bands can be readily assigned as combinations of the modes in Table 1, while the remainder are likely two-quanta combinations of a'' modes. For the purpose of supporting the identification of the carrier as *trans*-1VPR, however, assignments for the strongest bands are sufficient. Inspection of Table 1 reveals a far inferior match to *cis*-1VPR or 3VPR.

Further support for this assignment is provided by the simulation of the high resolution 462 nm band profile in the top half of Figure 3. The electronic transition is assigned as $\tilde{A}^2A''-\tilde{X}^2A''$. A rotational profile was computed for the near-

(41) Roberts, C.; Walton, J. C. *J. Chem. Soc., Perkin Trans. 2* **1981**, 553.
(42) MacInnes, I.; Walton, J. C. *J. Chem. Soc., Perkin Trans. 2* **1985**, 1073.

Table 2. Calculated Rotational Constants and Experimental T_0 Values (cm^{-1}) of the $\tilde{X}$ and $\tilde{A}$- States of *cis*- and *trans*-1VPR (CASSCF/6-31G*) Used in Simulations of the Rotational Profiles in Figure 3

	trans-1VPR	*cis*-1VPR
A''	1.3758	0.4502
B''	0.0792	0.1131
C''	0.0749	0.0904
A'	1.3044	0.4153
B'	0.0774	0.1138
C'	0.0732	0.0895
T_0	21644.6	21232.3
line width	0.10 cm^{-1}	0.14 cm^{-1}
band type	*a*-type	$a/b = 9$
T	25K	20K

prolate top *trans*-1VPR, with a purely *a*-type transition, as guided by a CASSCF calculation, using the asymmetric top simulation program ASYROTWIN.[43] The simulated profile, which is a near facsimile of the observed profile, was calculated using the $\tilde{X}$ and $\tilde{A}$ rotational constants (see Table 2) of *trans*-1VPR obtained directly from the CASSCF geometry optimizations, without alteration. The dispersed fluorescence spectra and rotational profile simulation thus strongly suggest that band *a* should be assigned to *trans*-1VPR. At 21 233 cm^{-1}, band *b* is just outside the spectral region scanned by Ding et al.[40] Also, it seems that none of the higher vibronic bands of this species that we observe in 2DF appear in their spectrum. However, we have confirmed that its carrier has mass 65 and below present strong evidence to assign band *b* as the origin transition of *cis*-1VPR.

***cis*-1-Vinylpropargyl Radical.** The DF spectrum b_1 appears to exhibit the same number of Franck−Condon active modes, at similar frequencies, as the *trans*-1VPR DF spectrum. In particular, the 2032 and 1503 cm^{-1} bands, which are very nearly coincident with those in the *trans*-1VPR spectrum, suggest that *cis*-1VPR and 3VPR, which contain double and triple bonds, should be leading candidates. We note that, as it contains the same chromophore as *trans*-1VPR, it is certainly reasonable to expect the *cis*-conformer to absorb nearby. This is borne out by calculations of the $\tilde{A}-\tilde{X}$ origin transition energies of *trans*-1VPR, *cis*-1VPR, and 3VPR. Absolute energies of the $\tilde{X}$ and $\tilde{A}$ states were calculated by MRCI. After including zero-point energies obtained from CASSCF vibrational frequencies, T_0 for *trans*-1VPR and *cis*-1VPR were calculated to be, respectively, 22 239 cm^{-1} (observed, 21 645 cm^{-1}) and 21 926 cm^{-1} (observed, 21 232 cm^{-1}), in good agreement with observation; the 3VPR origin is predicted to be significantly lower at 9198 cm^{-1}.

Returning to the DF spectrum b_1, we note that the agreement between the observed bands at 155, 373, and 642 cm^{-1} with the calculated frequencies $\nu_{17} = 153$ cm^{-1}, $\nu_{16} = 372$ cm^{-1}, and $\nu_{15} = 632$ cm^{-1} of *cis*-1VPR is much better than for *trans*-1VPR or 3VPR; the remaining assigned bands are also in remarkably close accord with calculated *cis*-1VPR frequencies. Further, as for *trans*-1VPR, we used ASYROTWIN to simulate the observed band profile *b*, employing the $\tilde{X}$ and $\tilde{A}$ state rotational constants of *cis*-1VPR without change from the CASSCF geometry optimizations (Figure 3). For *cis*-1VPR, which has a higher asymmetry splitting than the *trans*-conformer, a mixed 9:1 *a*/*b*-type transition was invoked. The choice of the ratio *a*/*b* was guided by the ratio of the square of the *a* and *b* components of the transition dipole moment of the $\tilde{A}-\tilde{X}$ electronic transition from the CASSCF calculation. The calculated rotational constants of *cis*- and *trans*-1VPR and those derived from the simulations, as well as the simulation parameters (line width, hybrid *a*/*b* character, and temperature) are contained in Table 2. We consider that the excellent agreement between the theoretical and experimental vibrational frequencies, rotational profiles, and transition energies strongly favor the assignment of the 471 nm band to *cis*-1VPR. Having by this stage formed the view that *cis*-1VPR was the most likely carrier, we further eliminated 3VPR (and any other isomer not explicitly considered here) from consideration by employing as a precursor pent-4-en-1-yne (H-1VPR), the molecular parent of 1VPR, with a hydrogen at the radical site (and which has also been observed in PIE of various hydrocarbon flames).[31] Using a very gentle discharge (low current and voltage) of this precursor, we were able to observe the DF spectra a_1 and b_1 with enhanced signal-to-noise, with *trans*-1VPR appearing slightly more abundant than the 471 nm band carrier.

In a low-current discharge of 1-hexyne, both 1VPR conformers can be easily formed by losing methyl radical, and then either eliminating molecular hydrogen or undergoing two H-abstraction steps. Little preference for *cis* or *trans* should be expected as there is little impediment to rotation about the relevant bond in the precursor, and further, the energy difference between the two isomers has been measured to be only 1.2 kJ/mol by electron spin resonance measurements.

Alternatively, cleavage of the C−C bond between the propargyl and the propyl moieties will yield the propargyl radical, which because of of the resonance stability is almost certainly the lowest energy channel. Propargyl radicals undergoing acetylene addition with a 1,3 hydrogen shift could yield the required structural isomer. Interestingly, in this case, a preference for the *trans* isomer should be observed. This may explain the apparent non-observation of *cis*-1VPR by Ding et al.[40] The reaction of propargyl with acetylene has been studied kinetically, although in that study the C_5H_5 products were not unambiguously determined.[44]

In comparison, to form 3VPR, the acetylene must add at the 3-position of propargyl, which possesses a lower radical density, which should at least result in its formation in much lesser quantities. Further, 3VPR is calculated to lie 13.4 kJ/mol above 1VPR.[33]

The relative energies of the two isomers and the height of the barrier between them were briefly investigated theoretically. A transition state (TS) search was performed by QST3 at the B3LYP/6-31G(d) level using the Gaussian03[38] suite of programs. A transition state was easily found and a frequency analysis for this structure indicated a single imaginary frequency, belonging to the torsional motion of the vinyl moiety about the C(1)−C(1′) bond, as expected. The zero-point energy of the TS was calculated to lie some 57 kJ/mol above the *trans* equilibrium geometry, in good agreement with the 54 kJ/mol measured by ESR,[42] while the *trans* isomer lies some 3.3 kJ/mol below the *cis*, a slightly larger figure than the 1.2 kJ/mol inferred from ESR.

Resonance Stability of 1-Substition of Propargyl. The assignment of these transitions to 1-vinylpropargyl isomers is consistent with what was observed for the phenylpropargyl analogues.[36] In that work, 1-phenylpropargyl (1PPR) was observed in abundance by LIF as a benzene discharge product;

(43) Judge, R. H.; Clouthier, D. J. *Comput. Phys. Commun.* **2001**, *135* (3), 293.

(44) Knyazev, V. D.; Slagle, I. R. *J. Phys. Chem. A* **2002**, *106*, 5613.

Table 3. Geometrical and Dynamical Parameters Indicating Resonance Stabilization[a]

	H-1VPR	1VPR	H-3VPR	3VPR
$r_{C\equiv C}$	1.202	1.215	1.208	1.237
$\nu_{C\equiv C}$	2135[b]	2025	2260	1985
$r_{C=C}$	1.329	1.365	1.339	1.358
$\nu_{C=C}$	1650[b]	1495	1613	1526
r_{1-2}	1.460	1.392	1.456	1.349
r_{v-p}	1.522	1.411	1.422	1.392

[a] As discussed in the text. Frequencies in cm^{-1} and bond lengths in Å. The bond length r_{v-p} is between the vinyl and propargyl moieties. [b] From ref 49.

no other reproducible resonant signal was observed corresponding to a $m/z = 115$ isomer in an extensive wavelength search. This was attributed to the unpaired electron in propargyl being situated primarily on the methylene moiety,[45,46] favoring 1PPR formation as a (mostly) secondary radical. Indeed, the resonance stabilization energy (RSE) of 1PPR (being almost the sum of the benzyl and propargyl RSEs) is 40 kJ/mol greater than that of 3PPR, which is only marginally greater than the RSE of propargyl itself,[47] inhibiting its further reaction once formed. This latter result is likely due to a combination of the increased delocalization furnished by concerted action of the propargyl and phenyl moieties in 1PPR, and the higher energy of 3-phenyl-1-propyne compared to 1-phenyl-1-propyne (respectively, the parent molecules of 1PPR and 3PPR), the latter of which is more highly conjugated. Similarly, the RSE of 3VPR measured from bond dissociation energies is 57 ± 14 kJ/mol which again is comparable to the RSE of propargyl itself,[48] while (insofar as such a comparison is appropriate) that of 1VPR measured by electron spin resonance (derived from the barrier to rotation between *cis* and *trans*) is 112 kJ/mol, which is close to the sum of the allyl and propargyl RSEs.[42] The causes of this are likely similar: the 3VPR parent (pent-4-en-2-yne, H-3VPR) is more highly conjugated, and therefore more stable, than the 1VPR parent (pent-4-en-1-yne, H-1VPR), while 1VPR is a more highly substituted, and therefore more stable radical, than 3VPR.

A comparison of the C−C bond lengths and vibrational frequencies in 1VPR and 3VPR with their molecular parents provides a simple, intuitive picture of the extent of resonance in each radical (Table 3). As a consequence of radical delocalization, one expects the vibrational frequencies and lengths of multiple bonds to decrease notably in going from the parent to the radical, and the opposite to be true for "single" bonds. In light of the above-mentioned RSEs, these changes should be more obviously confined to the propargyl moiety in 3VPR and spread more evenly throughout 1VPR, an interpretation that is largely borne out. C−C bond lengths of both parent molecules were obtained from B3LYP/6-311+G(d,p) geometry optimizations. A frequency calculation at the same level of theory was performed on the optimized H-3VPR geometry (scaled by 0.97, as for the radical), and vibrational frequencies of *syn* and *gauche* H-1VPR have recently been measured in the gas-phase.[49]

For 3VPR, the bond connecting the vinyl and the propargyl moieties is only slightly shorter than in H-3VPR (1.392 Å compared to 1.422 Å), reflecting as expected the extent of conjugation in the parent. The C=C double bond length is slightly (0.019 Å) longer in the radical, and the vibrational frequency drops by about 5%, from 1613 to 1526 cm^{-1}. By far the most obvious changes involve the propargyl moiety: the C(1)−C(2) bond length decreases from the parent to the radical by 0.11 Å, the C≡C bond increases by 0.03 Å, and the stretching frequency decreases remarkably, from 2260 to 1985 cm^{-1}, in close agreement with the corresponding frequency of the propargyl radical in the gas phase (1935 ± 15 cm^{-1}).[46] In light of this, it is not surprising that the RSE of 3VPR does not greatly exceed the propargyl RSE.

In contrast, in going from H-1VPR to *trans*-1VPR (similar results apply for the *cis*-conformer), the single bonds, C(1′)−C(1) and C(1)−C(2), which connect the double and triple bonds, shorten markedly, by 0.11 and 0.07 Å, respectively, and the frequencies of the stretching modes that most clearly involve these two bonds increase 30% from 847 and 930 cm^{-1} to 1100 and 1200 cm^{-1}. Further, the vinyl C=C bond lengthens by 0.036 Å, and the stretching frequency drops 10% from 1650 to 1495 cm^{-1}. Only the changes to the triple bond, though still significant, are less dramatic, with the length increasing by 0.013 Å and the stretching frequency dropping by about 5%, from 2135 to 2025 cm^{-1}. An ethynyl-substituted allyl radical may be an equally valid description of this species. Thus, while it may exceed expectation that the 1VPR RSE is near the sum of the propargyl and allyl RSEs, it is certainly reasonable to expect that it should significantly exceed either alone. We predict that, as further substituted propargyl radicals are identified in rarified chemical environments, a preponderance for substitution at the propargyl 1-position shall be exhibited.

Conclusion

Dispersed fluorescence spectra and high resolution LIF rotational profiles have been compared with vibrational frequencies and geometries from theoretical calculations to confirm the observation of the *cis*-1-vinylpropargyl and *trans*-1-vinylpropargyl radicals in a hydrocarbon discharge. These fundamental radical species are the second such 1-substituted propargyl radicals identified by our laboratory using the synergy of 2-dimensional fluorescence[36] and R2C2PI spectroscopies. These substituted propargyl radicals are implicated along with the propargyl radical itself in formation of aromatics in combustion, and planetary atmospheres. The spectra reported here provide the necessary probes to unambiguously study the role of C_5H_5 species in such environments.

Acknowledgment. This research was supported under the Australian Research Councils Discovery funding scheme (project nos. DP0665831 and DP0985767). N.J.R. acknowledges the University of Sydney for the award of a Gritton Scholarship. T.P.T. acknowledges the University of Sydney for a University Postgraduate Award, and N.C. acknowledges the award of an Endeavour International Postgraduate Research Scholarship from the Australian Government. K.N. acknowledges the Australian Research Council for an Australian Research Fellowship. We thank Prof. Y. Endo for computation resources.

Supporting Information Available: Full citations for refs 34, 38, and 39. This material is available free of charge via the Internet at http://pubs.acs.org.

JA904521C

(45) Tanaka, K.; Sumiyoshi, Y.; Ohshima, Y.; Endo, Y.; Kawaguchi, K. *J. Chem. Phys.* **1997**, *107*, 2728.
(46) Jochnowitz, E. B.; Zhang, X.; Nimlos, M. R.; Varner, M. E.; Stanton, J. F.; Ellison, G. B. *J. Phys. Chem. A* **2005**, *109*, 3812.
(47) Radom, L.; Menon, A. Private communication.
(48) Staker, W. S.; King, K. D.; Nguyen, T. T. *Int. J. Chem. Kinet.* **1992**, *24*, 781.
(49) Durig, J. R.; Zhu, X.; Guirgis, G. A.; Heldrich, F. J.; Wright, M. J. *J. Chem. Phys. A* **2003**, *107*, 8139.